source of disorder associated with the polyether loops in MOF-1001A, MOF-1001, and MOF-1002. Moreover, there is also the prospect of being able to construct chiral MOFs where the elements of chirality are planar (27) in origin.

17. V. Balzani, A. Credi, F. M. Raymo, J. F. Stoddart, *Angew. Chem. Int. Ed.* **39**, 3348 (2000).
18. S. J. Loeb, *Chem. Commun.* **2005**, 1511 (2005).
19. K. Kim, *Chem. Soc. Rev.* **31**, 96 (2002).
20. C.-F. Lee *et al.*, *Nature* **458**, 314 (2009).
21. Crystals of MOF-1001 were first immersed in acetone to exchange the *N,N*-dimethylformamide (DMF) guests and unreacted BPP34C10DA. This process was repeated nine times by decanting and refreshing with acetone (5 ml) every 30 min to ensure full exchange of DMF.
22. D. B. Amabilino *et al.*, *J. Am. Chem. Soc.* **117**, 11142 (1995).
23. P. R. Ashton, D. Philp, N. Spencer, J. F. Stoddart, *J. Chem. Soc. Chem. Commun.* **23**, 1677 (1991).
24. The experiments were done by introducing acetone-exchanged MOF-1001 into acetone solutions of PQT·2PF$_6$ with different amounts of PQT^{2+}. After sitting for 6 hours, solvent was then removed by evaporation and the residue was further dried under vacuum (10^{-2} torr) overnight at room temperature. A ^{15}N CP/MAS NMR spectrum was acquired on the solid sample and the loading of PQT^{2+} was determined by solution-state ^{1}H NMR spectroscopy after digestion of the solid. See (14).
25. H. K. Chae *et al.*, *Nature* **427**, 523 (2004).
26. K. Sonogashira, Y. Tohda, N. Hagihara, *Tetrahedron Lett.* **16**, 4467 (1975).
27. V. Prelog, G. Helmchen, *Angew. Chem. Int. Ed. Engl.* **21**, 567 (1982).
28. This work was supported by the U.S. Department of Defense (Defense Threat Reduction Agency grant HDTRA1-08-10023) and Northwestern University.

Fire As an Engineering Tool of Early Modern Humans

Kyle S. Brown,[1,2] Curtis W. Marean,[2] Andy I. R. Herries,[3,4] Zenobia Jacobs,[5] Chantal Tribolo,[6] David Braun,[1] David L. Roberts,[7] Michael C. Meyer,[5] Jocelyn Bernatchez[2]

The controlled use of fire was a breakthrough adaptation in human evolution. It first provided heat and light and later allowed the physical properties of materials to be manipulated for the production of ceramics and metals. The analysis of tools at multiple sites shows that the source stone materials were systematically manipulated with fire to improve their flaking properties. Heat treatment predominates among silcrete tools at ~72 thousand years ago (ka) and appears as early as 164 ka at Pinnacle Point, on the south coast of South Africa. Heat treatment demands a sophisticated knowledge of fire and an elevated cognitive ability and appears at roughly the same time as widespread evidence for symbolic behavior.

There is debate as to when modern human behavior appeared, although there is increasing evidence for symbolic behavior by 80 to 70 thousand years ago (ka) (1, 2) and perhaps earlier (3, 4), during the African Middle Stone Age (MSA, ~280 to 35 ka) (5). The MSA also displays tool traits that anticipate technologies occurring later in Eurasia. This includes the regular and sometimes predominant use of blade technology (4), the production of unmodified and backed bladelets for probable use in composite tools (6), the refinement of bifacial technology, the production of formal and standardized tool types (7), and the use of refined bone tools (8). Although most raw materials during the MSA came from local nearby sources, early modern humans expanded their use of fine-grained raw materials (exotics) (4, 9) from distant sources (10). The Still Bay [~71 to 70 ka (11) or earlier (12)] and Howiesons Poort (~65 to 60 ka) (11) MSA occurrences in South Africa display a preference for fine-grained materials, commonly silcrete [supporting online material (SOM) text] (13). The Still Bay occurrence has thin and symmetrical lanceolate and foliate shaped bifacials. The Howiesons Poort occurrence includes small retouched blade tools, along with the prepared-core and flake-and-blade technology typical of the MSA. The focus on silcrete has been argued to reflect functional need (14), increased mobility (9), trading networks (15), and even symbolic behavior (16).

Silcrete is traditionally described by archaeologists as a nonlocal fine-grained material that is highly workable in its natural state (4, 9, 17). However, our experimental replication using silcrete from sources on the south coast near Mossel Bay and Still Bay shows that these silcretes in their raw quarried form are difficult to flake consistently into formal tools. In Australia, indigenous knappers heated silcrete with fire (heat treatment) to improve the flaking quality of the material (18). Silcrete responds to heat treatment with significant improvement in workability and has a greater tolerance for high temperatures than do chert and flint (19). Following this lead, we found that heated South African silcrete is significantly more workable than unheated materials, and both bladelets and bifaces are easier to flake, with higher suc-cess rates. This transformation in workability is remarkably palpable when flaking both heated and unheated silcrete from the same source. Given these results, we undertook a systematic study of silcrete heat treatment and attempted to identify its presence or absence in the MSA.

We collected silcrete samples from sources located within 100 km of Pinnacle Point (20) (fig. S1). A witness control sample has been retained at our field laboratory in Mossel Bay, South Africa, for each nodule used in the experimental heat treatment study. Experimental silcrete samples were slowly heated to ~350°C in a scientific furnace or in sand beneath a fire pit (20).

The complexities of fracture mechanics make it difficult to quantify the workability of stone in a way that is relevant to human knapping (21). For this reason, we applied objective measures of workability and less objective but more realistic systematic flaking experiments. The rebound hardness test (22) assesses both the ability of a given rock mass to absorb energy and fracture predictability (SOM text). Rocks with internal flaws or low overall stiffness have lower rebound values (23). In these types of stones, the propagation of fracture will follow the internal structure of the rock rather than the direction of applied force. Heat-treated samples had significantly higher rebound hardness values (Wilcoxon matched-pairs test: $z = 2.512$, $P = 0.004$) than their paired untreated samples (fig. S2A and table S1) (20).

More carefully crafted bifacial tools have higher width-to-thickness ratios (W/T) (24), and variants of the W/T measurement correlate with projectile point function and ballistics (25). Timed heat-treated bifacial tool replications conducted by us had significantly higher W/T values [related-samples t test: $t(49) = 8.11$, $P < 0.001$] than their paired unheated bifaces (20). Using heated silcrete biface blanks, we could produce a significantly thinner biface that maximizes cutting edge, in the same amount of time needed to work the unheated bifaces (fig. S2, B and C). The heated biface samples closely resemble those of actual Still Bay point specimens (fig. S3). The rebound hardness and replication experiments combine to show that heat-treated silcretes consistently display more predictable fracture patterns, allowing

[1]Department of Archaeology, University of Cape Town, Rondebosch 7701, Cape Town, Republic of South Africa. [2]Institute of Human Origins, School of Human Evolution and Social Change, Post Office Box 872402, Arizona State University (ASU), Tempe, AZ 85287–4101, USA. [3]UNSW Archaeomagnetic Laboratory and Palaeosciences Laboratory, Integrative Palaeoecology and Anthropology Studies, School of Medical Sciences, University of New South Wales (UNSW), Kensington, New South Wales 2052, Australia. [4]Geomagnetism Laboratory, Department of Earth and Ocean Sciences, University of Liverpool, Liverpool L693BX, UK. [5]GeoQuEST Research Centre, School of Earth and Environmental Sciences, University of Wollongong, Wollongong 2522, Australia. [6]Institut de Recherche sur les Archéomatériaux–Centre de Recherche en Physique Appliquée à l'Archéologie, CNRS–Université de Bordeaux, Maison de l'Archéologie, Esplanade des Antilles, 33607 Pessac, France. [7]Council for Geoscience, Post Office Box 572, Bellville 7535, Republic of South Africa.

more efficient production of complex tool forms than do those that are not heat-treated.

Methods for recognizing intentionally heat-treated raw material have only been anecdotally applied to lithic technologies of similar age (SOM text). In some cases, burnt lithics are assumed to be deliberately heat-treated, when they could have been thermally altered unintentionally by bush fires, hearths, and the burning of the organic-rich sediments typical of caves. We suggest that arguments for intentional heat treatment must (i) be documented by at least two independent techniques for recognizing the heating, (ii) be applied to a statistically valid sample, and (iii) be from dated and unburned archaeological contexts where incidental heating is unlikely to have occurred.

We applied three independent methods [archaeomagnetism, thermoluminesence (TL), and maximum gloss (MG)] for recognizing heated silcrete from Pinnacle Point site 5-6 (PP5-6) after developing expectations from our work with experimentally heated and unheated silcrete samples. PP5-6 is one of a series of caves/rock shelters at Pinnacle Point (on the southern coast of South Africa) (3). We selected 26 piece-plotted silcrete artifacts for TL and magnetic analysis from five PP5-6 layers dated by optically stimulated luminescence dating to between ~47 and ~72 ka (Fig. 1 and table S2) from contexts showing no evidence for in situ burning as documented by field observations, micromorphology, and magnetic susceptibility of the sediments. Sample size was limited because the TL and magnetic analyses are destructive. An additional Still Bay biface from Blombos Sands was also analyzed (fig. S4). Nondestructive gloss analysis was performed on a larger sample (*n* = 153) of artifacts (table S3).

Our archaeomagnetic analyses included both mineral magnetic and palaeomagnetic approaches (20, 26). Mineral magnetic analysis identifies a consistent mineralogy for burnt versus unburnt sediment and lithic samples, because heating generally tranforms weaker magnetic minerals to stronger magnetic mineral phases at temperatures below ~600°C. Mineral magnetic analysis was conducted on all the deposits excavated from the site (SOM text). It indicates that the deposits from which the stone tools were recovered were not combustion features and do not contain any significant amount of burnt sediment (Fig. 1). As such, the stone tools are unlikely to have been burnt accidentally in the locations from which they were recovered.

Palaeomagnetic analysis identifies directional components of the natural remanent magnetization caused by different geological and anthropogenic factors (SOM text). An unheated rock will retain a geological remanence formed either during deposition, precipitation, or secondary chemical alteration. Heated rocks acquire a thermoremanent magnetization (TRM) if heated to above the Curie point of the remanence-carrying minerals (575°C for magnetite) (Fig. 2A) or a partial TRM (pTRM) if heated to below the Curie point. The thermomagnetic history of the rock can be

identified through stepwise incremental heating in the laboratory. The paleomagnetic vector method shows that all of the tested archaeological samples from PP5-6 (*n* = 12; some were too small for analysis) and the Still Bay biface from Blombos Sands (Fig. 2B) had been heated. Most samples had a single heating component with maximum temperatures between 300° to 400°C (table S4). This is a typical temperature range for anthropogenically burnt rocks and hearth stones from modern and South African prehistoric sites (26).

Electrons trapped in a mineral (such as quartz) under natural or artificial irradiation can be released when the mineral is heated (27), producing TL, whose intensity is related to the amount of trapped electrons (20). If the heating is high enough (for example, to 450°C for a few seconds), all the trapped electrons are released and the TL signal is zeroed. The TL signal grows again with the amount of applied irradiation. For geological samples, natural irradiation occurred for long enough to fully saturate the sample, as is the case with the unheated experimental samples (Fig. 2C). For the heated samples, the 0 dose signal is at the background level, and the 75- and 150-Gy dose signals increase with the applied dose. Our TL analyses of the archaeological samples confirm the findings

from mineral magnetics and show that all 26 samples were heated (Fig. 2D).

An increased reflectance [measured by a Novo Curve Glossmeter as gloss units (GU)] of the flaked surface is an indication of heat treatment in silcretes. This change is only visible on surfaces that are flaked after heat treatment (Fig. 3A). The flaked surfaces of heated experimental samples have significantly higher MG units than do those of unheated control samples [related-samples *t* test: $t(49) = 14.71$ $P < 0.001$] (20). Thus, a higher degree of gloss on archaeological materials documents that heat treatment occurred before tool production (SOM text). A sample of 153 silcrete lithics from PP5-6 and nearby PP13B was analyzed for gloss (table S3). The PP5-6 MG histograms for the SADBS (~71 to 72 ka) (fig. S5D) and DBCS (~60 to 65 ka) (Fig. 3) stratigraphic aggregates closely resemble that of the heated and flaked experimental samples, indicating that the majority of these archaeological samples exhibit gloss consistent with flaking after heat treatment. The sample histograms from the LBSR aggregate at PP5-6 (~79 to 86 ka) (fig. S5E) and LCMSA aggregate of PP13B (~164 ka) (Fig. 3) fall between the unheated and heated experimental data sets but do contain specimens with MG values above the experimental threshold for unheated
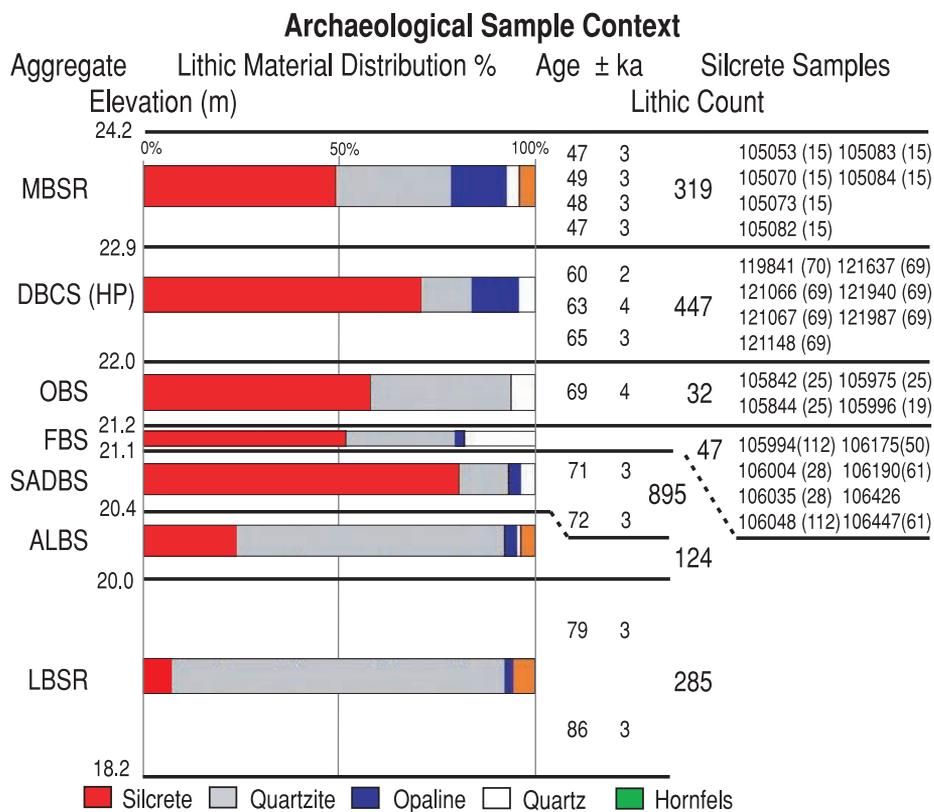

Fig. 1. Age (in thousands of years) and stratigraphic context for archaeological heat-treated samples from PP5-6. Raw material bar graphs are provided for each stratigraphic aggregate (see SOM text for complete description of PP5-6 stratigraphy) to show change in lithic raw materials used through time. Elevation is in meters above mean sea level, and age was determined by Optically Stimulated Luminescence dating (SOM text). Lithic count is the number of piece-plotted artifacts cataloged to date. Magnetic susceptibility values in parentheses after the sample specimen numbers provide an estimate of the potential for incidental burning (SOM text).

silcrete, indicating that some artifacts from these older layers were flaked from heated silcrete (Fig. 3 and fig. S5).

Heat treatment provides the option of exploiting more-local but poorer raw materials and compensating by improving their quality (*28*). Heat treatment front-loads tool production costs by forcing the toolmaker to invest in fire production in order to improve the subsequent knapping process. This practice may only become economically advantageous when fuel is abundant or when social conditions restrict access to preferred raw materials.

The controlled use of fire was a breakthrough invention that allowed cooking, the production of warmth and light, and protection from predators (*29*). Evidence of cooking extends back to 790 ka

(*30*), and eventually fire was used for more complex technologies such as firing clay for ceramics and heating ores for metallurgy. However, the technological links between using fire for simple tasks of light and heat production and using it as an engineering tool to alter raw materials remain poorly documented and understood. Heat treatment and its requirements signal an important technological advance, in that fire was now being carefully manipulated as an engineering tool.

Starting around ~71 ka in South Africa, there is recurrent evidence for early symbolic behavior and complex technologies that predate their occurrence outside Africa. Our results at PP5-6 show that at this same time, early modern humans regularly employed pyrotechnology to in-

crease the quality and efficiency of their stone tool manufacture process. This technology required in these early humans a novel association between fire, its heat, and a structural change in stone with consequent flaking benefits that may signal a complex cognition. Our gloss analysis of the PP13B lithics suggests that this technology may have originated by 164 ka. Heat-treatment technology in Africa may explain the presence of advanced tools in the African MSA and their rarity in the Eurasian Middle Paleolithic, where Neanderthals predominated. As these early modern humans moved into Eurasia, the ability to alter and improve available raw materials and increase the quality and efficiency of stone tool manufacture may have been a behavioral advantage.
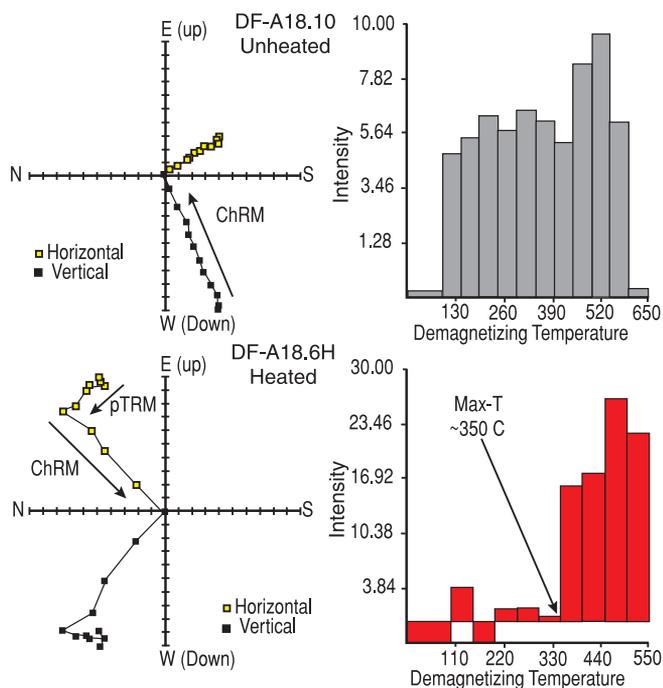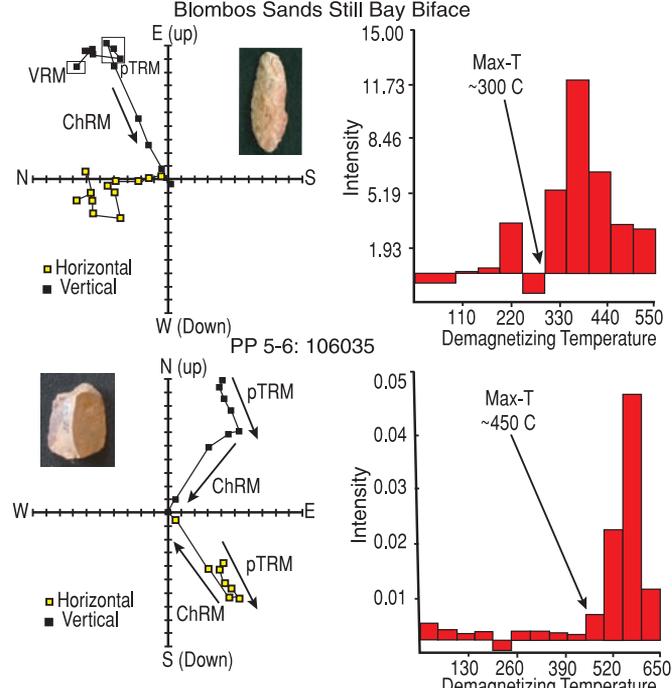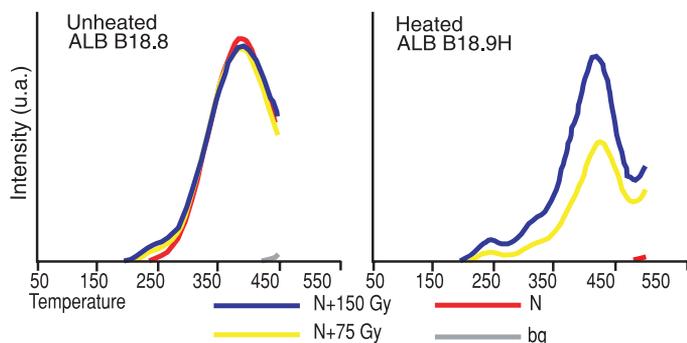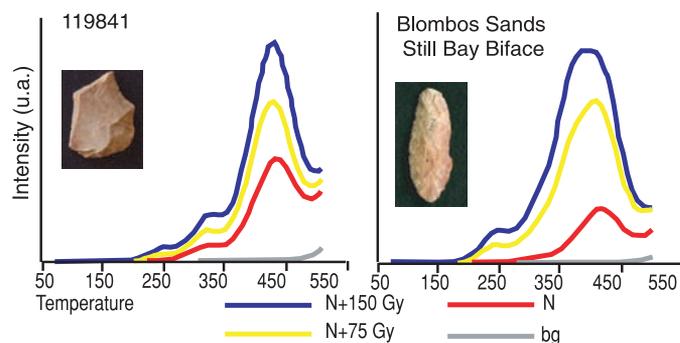

Fig. 2. Archaeomagnetic and thermoluminescence graphs of heated and unheated stone from experimental and archaeological samples. (**A**) The unheated specimen (top) shows a weak single-component geological remanence (ChRM). The heated experimental sample (bottom) shows a two-component signal that includes the remanent ChRM and pTRM from the heating process. The maximum temperature of heating has been reached at ~300°C in this sample. (**B**) The Still Bay point (top) and Howiesons Poort flake (bottom) samples show a multicomponent signal, with the pTRM from the heating event being removed at ~350° and 450°C, respectively. (**C**) TL has not been zeroed on the untreated experimental sample (left) and is fully saturated (no increase of the signal with dose). The TL signal increased with the given dose on the heated experimental sample (right). (**D**) The archaeological samples resemble the unsaturated, heated experimental samples, because the TL signal still increases with the given dose.
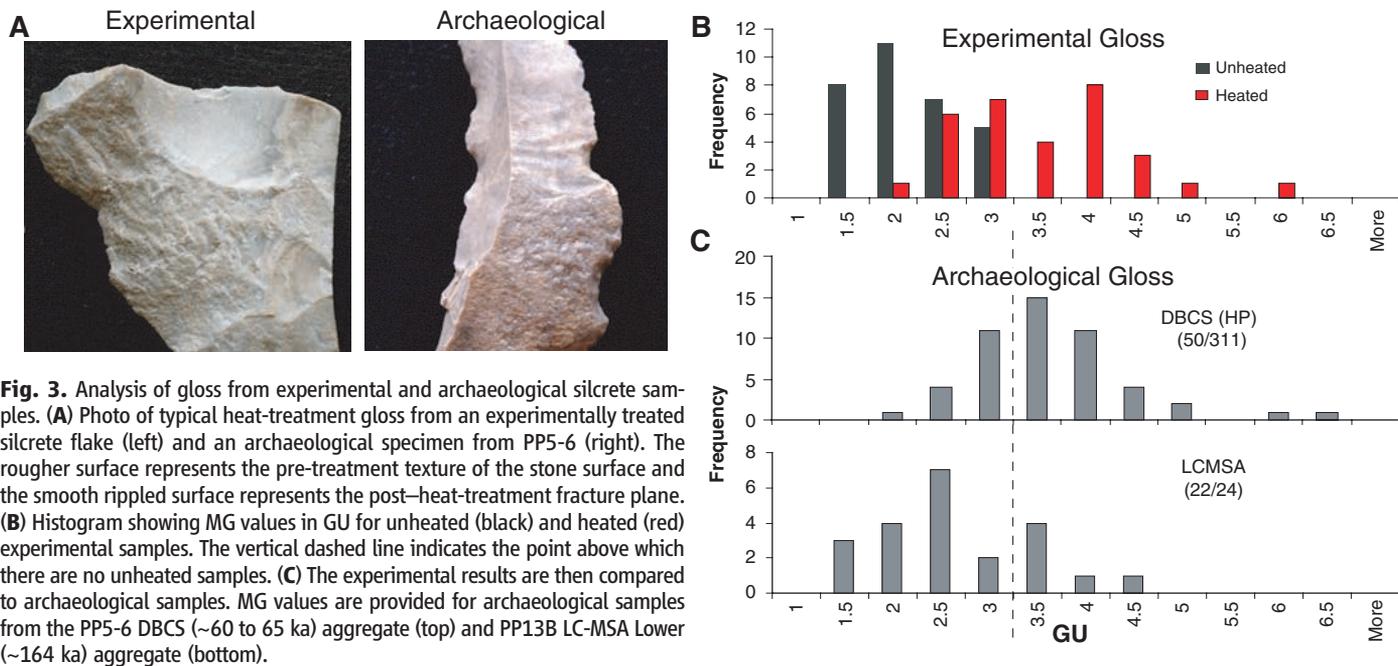
A

Experimental | Archaeological

B

Experimental Gloss

C

Archaeological Gloss

DBCS (HP)
(50/311)

LCMSA
(22/24)

GU

Fig. 3. Analysis of gloss from experimental and archaeological silcrete samples. (**A**) Photo of typical heat-treatment gloss from an experimentally treated silcrete flake (left) and an archaeological specimen from PP5-6 (right). The rougher surface represents the pre-treatment texture of the stone surface and the smooth rippled surface represents the post–heat-treatment fracture plane. (**B**) Histogram showing MG values in GU for unheated (black) and heated (red) experimental samples. The vertical dashed line indicates the point above which there are no unheated samples. (**C**) The experimental results are then compared to archaeological samples. MG values are provided for archaeological samples from the PP5-6 DBCS (~60 to 65 ka) aggregate (top) and PP13B LC-MSA Lower (~164 ka) aggregate (bottom).

References and Notes

1. F. d'Errico *et al.*, *J. Hum. Evol.* **48**, 3 (2005).
2. C. S. Henshilwood *et al.*, *Science* **295**, 1278 (2002).
3. C. W. Marean *et al.*, *Nature* **449**, 905 (2007).
4. S. McBrearty, A. S. Brooks, *J. Hum. Evol.* **39**, 453 (2000).
5. C. A. Tryon, S. McBrearty, *J. Hum. Evol.* **42**, 211 (2002).
6. M. Lombard, *J. Hum. Evol.* **53**, 406 (2007).
7. J. D. Clark, *J. World Prehist.* **2**, 235 (1988).
8. C. S. Henshilwood *et al.*, *J. Hum. Evol.* **41**, 631 (2001).
9. S. H. Ambrose, K. G. Lorenz, in *The Emergence of Modern Humans: An Archaeological Perspective*, P. Mellars, Ed. (Edinburgh Univ. Press, Edinburgh, 1990), pp. 3–33.
10. H. V. Merrick, F. H. Brown, W. P. Nash, in *Society, Culture, and Technology in Africa*, S. T. Childs, Ed. (Univ. of Pennsylvania Museum of Archaeology and Anthropology, Philadelphia, PA, 1994), pp. 29–44.
11. Z. Jacobs *et al.*, *Science* **322**, 733 (2008).
12. C. Tribolo *et al.*, *J. Archaeol. Sci.* **36**, 730 (2009).
13. T. P. Volman, in *Southern African Prehistory and Paleoenvironment*, R. G. Klein, Ed. (Balkema, Rotterdam, Netherlands, 1984), pp. 169–220.
14. A. J. Mackay, *Archaeol. Sci.* **35**, 614 (2008).
15. H. J. Deacon, in *The Human Revolution*, P. Mellars, C. Stringer, Eds. (Princeton Univ. Press, Princeton, NJ, 1989), pp. 547–564.
16. S. Wurz, *S. Afr. Archaeol. Bull.* **54**, 38 (1999).
17. G. S. McCall, *J. Archaeol. Sci.* **34**, 1738 (2007).
18. M. Hanckel, *Arch. Oceania* **20**, 98 (1985).
19. J. A. Webb, M. Domanski, *Archaeometry* **50**, 555 (2008).
20. Materials and methods are available as supporting material on *Science* Online.
21. A. W. Pelcin, *J. Archaeol. Sci.* **24**, 749 (1997).
22. A. Goudie, *Prog. Phys. Geogr.* **30**, 703 (2006).
23. M. Fener *et al.*, *Rock Mech. Rock Eng.* **38**, 329 (2005).
24. E. Callahan, *Arch. Eastern North America* **7**, 1 (1979).
25. J. J. Shea, *J. Archaeol. Sci.* **33**, 823 (2006).
26. A. I. R. Herries, in *Australian Archaeometry*, A. Fairbrain, S. O'Conner, Eds. (Australian National Univ. Press, Canberra, Australia, 2009), pp. 235–253.
27. M. J. Aitken, *Thermoluminescence Dating* (Academic Press, London, 1985).
28. J. J. Flenniken, J. P. White, *Aust. Aborig. Stud.* **1**, 43 (1983).
29. J. D. Clark, J. W. K. Harris, *Afr. Archaeol. Rev.* **3**, 3 (1985).
30. N. Goren-Inbar *et al.*, *Science* **304**, 725 (2004).
31. We thank the Institute for Social Science Research staff at ASU and the Mossel Bay Archaeology Project staff for their

Mesotocin and Nonapeptide Receptors Promote Estrildid Flocking Behavior

James L. Goodson,* Sara E. Schrock, James D. Klatt, David Kabelik, Marcy A. Kingsbury

Proximate neural mechanisms that influence preferences for groups of a given size are almost wholly unknown. In the highly gregarious zebra finch (Estrildidae: *Taeniopygia guttata*), blockade of nonapeptide receptors by an oxytocin (OT) antagonist significantly reduced time spent with large groups and familiar social partners independent of time spent in social contact. Opposing effects were produced by central infusions of mesotocin (MT, avian homolog of OT). Most drug effects appeared to be female-specific. Across five estrildid finch species, species-typical group size correlates with nonapeptide receptor distributions in the lateral septum, and sociality in female zebra finches was reduced by OT antagonist infusions into the septum but not a control area. We propose that titration of sociality by MT represents a phylogenetically deep framework for the evolution of OT's female-specific roles in pair bonding and maternal functions.

Sociality, as defined by modal species-typical group size, is a core component of social organization that strongly affects reproductive behavior, disease transmission, resource exploitation, and defense (*1, 2*). However, the neural mechanisms that titrate sociality and regulate the preference to live as singletons, in large groups, or somewhere in between are largely unknown. This likely reflects limited tractability, partly because the space requirements of large species-typical group sizes may be difficult to accommodate in experimental settings and, more importantly, because the behavioral dimension of sociality is difficult to isolate in comparative studies. For instance, because rodent species that differ in sociality also tend to differ in mating system, patterns of parental care, and other aspects of behavior and ecology that can influence neural and endocrine mechanisms associated with sociality (*3, 4*), comparative studies are not

Department of Biology, Indiana University, Bloomington, IN 47405, USA.

*To whom correspondence should be addressed. E-mail: jlgoodso@indiana.edu